C. R. Chimie 16 (2013) 451–461

Contents lists available at SciVerse ScienceDirect

Comptes Rendus Chimie

www.sciencedirect.com

Full paper/Mémoire

Carboxylic-supported copper complexes as catalyst for the green oxidative coupling of 2,6-dimethylphenol: Synthesis, characterization and structure

Qi Liu [a,*], Huai Guang Wu [b]

[a] Jiangsu Key Laboratory of Agricultural Meteorology and the College of Computer and Software, Nanjing University of Information Science and Technology, 210044 Nanjing, People's Republic of China

[b] Zhengzhou University of Light Industry, Zhengzhou, 450002 Henan, People's Republic of China

ARTICLE INFO

Article history:
Received 20 June 2012
Accepted after revision 20 November 2012
Available online 5 January 2013

Keywords:
Copper(II) complexes
Oxidative coupling
Heterogeneous catalyst
Green chemistry

ABSTRACT

Three new Cu(II) complexes with carboxylic ligand, namely $\{[Cu(qc)_2(py)]\cdot 4H_2O\}_\infty$ (**1**), $[Cu(qc)_2(4,4'\text{-bpy})]_\infty$ (**2**) and $[Cu(pc)(2,2'\text{-bpy})(H_2O)]_2\cdot H_2O$ (**3**) (Hqc = 3-hydroxy-2-quinoxalinecarboxylic acid, H_2pc = 4-hydroxyphthalic acid, py = pyrazine) have been synthesized and characterized. In both **1** and **2**, each Cu(II) ion is coordinated by two quinoxalinecarboxylate moieties in the equatorial plane and two 4,4′-bpy or pyrazine units provide coordination in the axial positions, thus, resulting in a 1-D polymeric chain structure. Complex **3** has a dimeric structure in which two Cu(II) cations are bridged by two deprotonated pc^{2-} ligands and two 2,2′-bpy molecules. As heterogeneous catalysts, the title complexes showed high catalytic efficiency in the green oxidative polymerization of 2,6-dimethylphenol (DMP) to poly(1,4-phenylene ether) (PPE) in the presence of H_2O_2 as oxidant in water under mild conditions. Moreover, they allow reuse without significant loss of activity through four runs, which suggests that these catalysts are efficient, mild, and easily recyclable for the oxidative coupling of DMP. The preliminary study of the catalytic–structural correlations suggests that the coordination environment of the metal center plays an important role in the improvement of their catalytic efficiencies.

1. Introduction

In the past decades, metal–organic complexes, in which the metal centers are interconnected by organic linkers to display a variety of supramolecular architectures, have attracted great attention due to their diverse structural topologies and potential applications in areas of catalysis and materials science [1,2]. In the specific case of catalysis, the unique characteristic of the Cu^{II}/Cu^{I} redox couple renders many of their complexes suited for various catalysis reactions [3], especially for the green catalysis process since copper is a cheap and minor toxic metal.

Poly(1,4-phenylene ether) (PPE) as an engineering plastic has been widely used in various areas, such as business equipment and the electrical and automotive industries. The oxidative polymerization of 2,6-dimethylphenol (DMP) to form PPE was first carried out by Hay and his GE group in 1959 with a copper–pyridine complex as a catalyst in a nitrobenzene solution [4]. Along with the formation of PPE by C–O coupling, an undesirable by-product, 3,3′,5,5′-tertramethyl-4,4′-diphenoquinone (DPQ), was also produced by the C–C coupling of two monomeric phenols. Although the oxidative polymerization of DMP in organic solvents has provided a convenient method for manufacturing PPE in industry, both a solvent-recovery process and an antiexplosive reactor are required in industrial PPE production [5]. From the view of green chemistry, the use of water as a reaction medium is considered environmentally friendly and PPE can easily

* Corresponding author.
E-mail address: qrankl@163.com (Q. Liu).

1631-0748/$ – see front matter © 2012 Académie des sciences. Published by Elsevier Masson SAS. All rights reserved.
http://dx.doi.org/10.1016/j.crci.2012.11.011

be separated from water due to its insolubility in water [6,7]. In 2004, Nishide et al. first used potassium ferricyanide as an oxidant to synthesize PPE in alkaline water. Unfortunately, the use of potassium ferricyanide is still environmentally deleterious [8]. So far, the green oxidative coupling of DMP in environmental friendly solvents with clean oxidants is studied extremely rarely. Therefore, this reaction is still a research field of great challenge from the standpoint of "green chemistry and technology". Meantime, it is extraordinarily desired that the development of efficient catalysts suited for the milder "green" conditions, and the investigation of catalytic–structural correlations, which have great importance for the exploitation of new catalysts. For the purpose of replacing the traditional organic-medium systems by environmental friendly processes, we have prepared three new copper carboxylic adducts $\{[Cu(qc)_2(py)]\cdot 4H_2O\}_\infty$ (**1**), $[Cu(qc)_2(4,4'\text{-bpy})]_\infty$ (**2**) and $[Cu(pc)(2,2'\text{-bpy})(H_2O)]_2\cdot H_2O$ (**3**) (Hqc = 3-hydroxy-2-quinoxalinecarboxylic acid, H_2pc = 4-hydroxyphthalic acid, py = pyrazine) and explored their application as catalysts for an aqueous-medium catalysis process of the oxidative coupling of DMP by using hydrogen peroxide as oxidant under mild conditions.

2. Experimental

2.1. General information and materials

All the solvents and chemicals (analytical grade) were used without further purification. 3-Hydroxy-2-quinoxalinecarboxylic acid (Hqc), 4-hydroxyphthalic acid (H_2pc), pyrazine (py), 4,4′-bpy, 2,2′-bpy and 2,6-dimethylphenol (DMP) (99% pure) were used as obtained from J&K Chemical Ltd. Elemental analyses (C, H, and N) were performed on a Perkin-Elemer 240C analyzer. The IR spectra were recorded in the range 4000–400 cm^{-1} on a Tensor 27 OPUS (Bruker) FT-IR spectrometer with KBr pellets. The X-ray powder diffraction patterns (XRPD) were recorded on a Rigaku D/Max-2500 diffractometer, operated at 40 kV and 100 mA, using a Cu-target tube and a graphite monochromator. The intensity data were recorded by continuous scan in a $2\theta/\theta$ mode from 3° to 80° with a step size of 0.02° and a scan speed of 8° min^{-1}.

2.2. Synthesis of $\{[Cu(qc)_2(py)]\cdot 4H_2O\}_\infty$ (1)

To a stirred solution of $Cu(ClO_4)_2\cdot 6H_2O$ (18.75 mg, 0.05 mmol) in H_2O (2 mL) was added 1 equiv. of pyrazine (4 mg, 0.05 mmol) in CH_3OH (5 mL). This was stirred for 5 min, and then a 5 mL CH_3OH solution of 3-hydroxy-2-quinoxalinecarboxylic acid (9.5 mg, 0.05 mmol) was added to the reaction mixture and then filtered to give a green solution. Slow evaporation of the solvent at room temperature gave rise to green block single crystals suitable for X-ray single-crystal analysis after ca 5 days. Yield: ~ 40% (based on Cu). Anal. calcd for $C_{22}H_{20}CuN_6O_{10}$: C, 44.64; H, 3.41; N, 14.20%. Found: C, 44.58; H, 3.49; N, 14.27%; IR (KBr)/cm^{-1}: 3464(m), 1683(s), 1609(m), 1374(m), 1326(m), 1221(w), 986(w), 882(w), 806(w), 776(m), 676(m), 446(w).

2.3. Synthesis of $[Cu(qc)_2(4,4'\text{-bpy})]_\infty$ (2)

To a stirred solution of 2 equiv. of $Cu(ClO_4)_2\cdot 6H_2O$ (37.5 mg, 0.1 mmol) in H_2O (5 mL) were added 2 equiv. of 4,4′-bpy (15.6 mg, 0.1 mmol) in CH_3OH (5 mL). After stirring for 5 min, a solution of 3-hydroxy-2-quinoxalinecarboxylic acid (19.0 mg, 0.1 mmol) in CH_3OH (5 mL) was added, and the mixture was then stirred for 10 min. Upon evaporation of the solvent, the green block crystals were isolated in 50% yield. Anal. calcd for $C_{28}H_{16}CuN_6O_6$: C, 56.43; H, 2.71; N, 14.10%. Found: C, 56.51; H, 2.79, N 13.98%; IR (KBr)/cm^{-1}: 3434(w), 1645(s), 1543(m), 1448(s), 1348(m), 1285(w), 1145(w), 1076(w), 879(w), 739(w), 552(m), 439(w).

2.4. Synthesis of $[Cu(pc)(2,2'\text{-bpy})(H_2O)]_2\cdot H_2O$ (3)

A mixture containing $Cu(ClO_4)_2\cdot 6H_2O$ (37.5 mg, 0.1 mmol), NaOH (4 mg, 0.1 mmol), 4-hydroxyphthalic acid (9.1 mg, 0.05 mmol), 2,2′-bpy (7.8 mg, 0.05 mmol) and water (10 mL) was placed inside a Teflon-lined stainless steel vessel (20 mL). It was heated to 120 °C for 48 h under autogenous pressure and then cooled to room temperature at a rate of 5 °C/h. The reaction solution was filtered and left to stand undisturbed. Blue block single crystals suitable for X-ray analysis were obtained after a period of 1 week in a yield of 68%. Anal. calcd for $C_{18}H_{16}CuN_2O_7$: C, 49.60; H, 3.70; N, 6.43%. Found: C, 49.71; H, 3.58; N, 6.37%; IR(KBr, cm^{-1}): 3507(m), 3083(m), 2680(w), 1551(s), 1389(s), 1306(m), 1266(m), 1161(w), 1066(w), 874(m), 729(m), 635(w), 452(w).

2.5. General procedure for the catalytic oxidative coupling of 2,6-dimethylphenol

All of the polymerizations were carried out in a 10 mL, three-necked, round-bottom reaction flask fitted with a water condenser. One neck of the flask was equipped with a mercury thermometer for measuring the reaction temperature. The crystal complex catalysts were ground well into appropriate sizes to increase the surface area, but not too small for a convenient filtration (the average particle size of 10–12 μm). DMP (122 mg, 1 mmol) was dissolved in water (5 mL). The 1.5 mol % complex was added to the solution, and the mixture was vigorously stirred under air at 40 °C. Then, hydrogen peroxide (30% aqueous solution) was slowly added into the mixture using a microinjector every 15 min for two times to minimize H_2O_2 decomposition. After 4 h, the reaction was stopped and the polymer product appeared as an off-white powder after salting out by the addition of sodium chloride (1.17 g, 0.02 mol). Then the mixture was transferred into a separatory funnel, the organic materials were extracted after the addition of a few milliliters of CH_2Cl_2. This was repeated three times. The combined organic extracts were dried with anhydrous $MgSO_4$ and the solvent, after filtration, was evaporated in vacuo. The products were separated by preparative TLC performed on dry silica gel plates with ethyl ether–petroleum ether (1:3 v/v) as the developing solvents. PPE and DPQ were collected and dried in vacuo. We also can get the polymeric products by the simple filtration after salting out, followed by the reprecipitation from chloroform to methanol.

Table 1
Crystal data and structure refinement for $\{[Cu(qc)_2(py)]\cdot 4H_2O\}_\infty$ (**1**), $[Cu(qc)_2(4,4'\text{-bpy})]_\infty$ (**2**) and $[Cu(pc)(2,2'\text{-bpy})(H_2O)]_2\cdot H_2O$ (**3**).

	1	2	3
Formula	$C_{22}H_{20}CuN_6O_{10}$	$C_{28}H_{16}CuN_6O_6$	$C_{18}H_{16}CuN_2O_7$
Formula weight	591.98	596.01	435.87
Crystal system	Triclinic	Orthorhombic	Orthorhombic
Space group	P-1	Fdd2	Pbcn
a (Å)	6.9911(4)	11.1387(4)	20.5311(16)
b (Å)	8.9006(4)	12.2921(4)	11.1914(8)
c (Å)	10.3196(5)	35.3173(16)	15.4446(12)
α (°)	86.613(4)	90	90.00
β (°)	71.990(4)	90	90.00
γ (°)	76.660(4)	90	90.00
V (Å^3)	594.14(5)	4835.6(3)	3548.7(5)
T (K)	293(2)	293(2)	296(2)
Z	1	8	8
μ (Mo Kα) (cm^{-1})	0.991	1.637	1.277
Number of reflections collected [$I > 2\delta(I)$]	3742	9997	12223
Number of independent reflections	2203	2201	3296
Final R^a, $R_w{}^b$	0.0387, 0.0986	0.0236, 0.0588	0.0417, 0.1011

[a] $R = \sum\|F_o|-|F_c\|/\sum|F_o|$.

[b] $R_w = \left[\sum(\|F_o|-|F_c\|)2/\sum_w|F_o|^2\right]^{1/2}$.

The following is the standard procedure for the homogeneous oxidation: the crystal complex catalysts were powdered to increase the surface area for the catalysts homogeneous prior to use. Under air, the substrate 2,6-dimethylphenol (0.122 g, 1 mmol) was dissolved in the 1:1 (v/v, 5 mL) mixture of methanol–toluene in a 10 mL flask, and a 0.5% molar ratio of catalyst/substrate and a 5 molar ratio of NaOMe/catalyst were added to above solution with a magnetic stirrer. Then, hydrogen peroxide (30% aqueous solution) was slowly added into the mixture using a syringe pump every 15 min 10 μl for five times to minimize H_2O_2 decomposition. After 2 h, the sample was concentrated in vacuo, and the products were separated by preparative TLC performed on dry silica gel plates. All reactions were run in duplicate, and the data reported represent the average of these reactions.

Poly(phenylene ether) (PPE): ^{1}H NMR ($CDCl_3$, TMS) $\delta = 6.44$ (s, 2H; H_{Ar}), 2.09 ppm (s, 6H; CH_3); ^{13}C NMR ($CDCl_3$, TMS) $\delta = 16.6$–16.8, 114.1, 114.5, 124.4, 125.0, 129.0, 131.6, 132.7, 145.6, 146.4, 151.5, 154.5, 154.8 ppm; IR (KBr): $\overline{\nu}_{C\text{-}O\text{-}C} = 1186\ \ \mathrm{cm}^{-1}$.

Diphenoquinone (DPQ): ^{1}H NMR ($CDCl_3$, TMS) $\delta = 8.2$ (s, 4H), 7.1 (s, 2H), 2.1 ppm (12H); ^{13}C NMR ($CDCl_3$, TMS) $\delta = 17.07$, 129.56, 135.67, 139.10, 187.21 ppm; IR (KBr): $\overline{\nu}_{C=O} = 1594\ \ \mathrm{cm}^{-1}$.

2.6. X-ray structure analyses

X-ray single-crystal diffraction measurements for complexes **1**–**3** were carried out on a Bruker Smart 1000 CCD diffractometer equipped with a graphite crystal monochromator situated in the incident beam for data collection at 293(2) K. The determinations of unit cell parameters and data collections were performed with Mo-Kα radiation (λ = 0.71073 Å) and unit cell dimensions were obtained with least-square refinements. The program SAINT [9] was used for integration of the diffraction profiles. Semi-empirical absorption corrections were applied using SADABS program [10]. All the structures were solved by direct methods using the SHELXS program of the SHELXTL package and refined with SHELXL [11]. Metal atoms in each complex were located from the E-maps, and other non-hydrogen atoms were located in successive difference Fourier syntheses and refined with anisotropic thermal parameters on $|F|^2$. The hydrogen atoms were added theoretically, riding on the concerned atoms and refined with fixed thermal factors. Crystal data and structure refinement of complexes **1**–**3** are summarized in Table 1. Selected bond lengths and bond angles are listed in Table 2.

3. Results and discussion

3.1. Crystal structure of $\{[Cu(qc)_2(py)]\cdot 4H_2O\}_\infty$ (1)

Crystallographic analysis reveals that **1** crystallizes in the triclinic space group P-1 with the compositions of one neutral asymmetric unit $[Cu(qc)_2(py)]$ and four lattice water molecules, and assumes an infinite 1-D chain array. As illustrated in Fig. 1, the Cu(II) ion, being located at an inversion center, is six-coordinated by two nitrogen atoms (N1, N1A) and two oxygen atoms (O2, O2A) from different qc^- ligands and a pair of nitrogen donors (N3, N3A) from two pyrazine molecules in a nearly ideal octahedron with N1, N1A, O2, O2A composing the basal plane (the mean deviation from plane of 0 Å) and N3, N3A holding the axial positions. Although the ligand is deprotonated, only the quinolinecarboxylate group is involved in metal coordination. Each deprotonated qc^- ligand serves as a two-connected node to coordinate with the Cu(II) atom through its nitrogen of quinoxaline and carboxylate in monodentate mode. The bond angles around Cu(II) ion vary from 76.28 (7) to 180.0°. The Cu-O bond lengths are 1.9206 (17) Å, and the Cu-N bond lengths are in the range 2.094 (2)–2.400 (2) Å, which are comparable to those observed for $\{[Cu(btp)(HBTC)_2]_3\cdot 0.5H_2O\}_n$ and $[Cu(btmb)(HBTC)]_n$

Table 2
Selected bond distances (Å) and bond angles (°).

$\{[Cu(qc)_2(py)]\cdot 4H_2O\}_\infty$ (**1**)					
Bond distances					
Cu1-O2	1.9214(18)	Cu(1)-O(2)#1	1.9214(18)	Cu1-N1	2.400(2)
Cu(1)-N(1)#1	2.400(2)	Cu1-N3	2.095(2)	Cu(1)-N(3)#1	2.095(2)
Bond angles					
O(2)#1-Cu(1)-O(2)	180.0	O(2)#1-Cu(1)-N(3)#1	89.95(8)	O(2)-Cu(1)-N(3)#1	90.05(8)
O(2)#1-Cu(1)-N(3)	90.05(8)	O2-Cu1-N3	89.95(8)	N(3)#1-Cu(1)-N(3)	180.00(12)
O(2)#1-Cu(1)-N(1)	103.74(7)	O(2)-Cu(1)-N(1)	76.26(7)	N(3)#1-Cu(1)-N(1)	89.86(8)
N(3)-Cu(1)-N(1)	90.14(8)	O(2)#1-Cu(1)-N(1)#1	76.26(7)	O(2)-Cu(1)-N(1)#1	103.74(7)
N(3)#1-Cu(1)-N(1)#1	90.14(8)	N(3)-Cu(1)-N(1)#1	89.86(8)	N(1)-Cu(1)-N(1)#1	180.00(10)
$[Cu(qc)_2(4,4'\text{-bpy})]_\infty$ (**2**)					
Bond distances					
Cu1-O2	1.9165(18)	Cu(1)-O(2)#1	1.9909(14)	Cu(1)-N(3)	2.031(4)
Cu(1)-N(4)#2	2.040(4)	Cu(1)-N(1)#1	2.3611(18)	Cu(1)-N(1)	2.3611(18)
Bond angles					
O(2)-Cu(1)-O(2)#1	176.57(11)	O(2)-Cu(1)-N(3)	91.71(5)	O(2)#1-Cu(1)-N(3)	91.71(5)
O(2)-Cu(1)-N(4)#2	88.29(5)	O(2)#1-Cu(1)-N(4)#2	88.29(5)	N(3)-Cu(1)-N(4)#2	180.0
O(2)-Cu(1)-N(1)#1	103.11(6)	O(2)#1-Cu(1)-N(1)#1	76.98(6)	N(3)-Cu(1)-N(1)#1	88.50(6)
N(4)#2-Cu(1)-N(1)#1	91.50(6)	O(2)-Cu(1)-N(1)	76.98(6)	O(2)#1-Cu(1)-N(1)	103.11(6)
N(3)-Cu(1)-N(1)	88.50(6)	N(4)#2-Cu(1)-N(1)	91.50(6)	N(1)#1-Cu(1)-N(1)	177.01(12)
$[Cu(pc)(2,2'\text{-bpy})(H_2O)]_2\cdot H_2O$ (**3**)					
Bond distances					
Cu1-O2	1.952(2)	Cu1-O1	1.960(2)	Cu1-N2	1.992(3)
Cu1-N1	1.994(3)	Cu1-O6	2.186(2)		
Bond angles					
O2-Cu1-O1	91.75(10)	O2-Cu1-N2	93.23(11)	O1-Cu1-N2	162.76(11)
O2-Cu1-N1	174.41(12)	O1-Cu1-N1	92.81(11)	N2-Cu1-N1	81.48(13)
O2-Cu1-O6	89.15(10)	O1-Cu1-O6	99.18(10)	N2-Cu1-O6	97.39(11)
N1-Cu1-O6	93.30(11)				

(btp = 1,3-bis(1,2,4-triazol-1-yl)propane, btmb = 4,4′-bis(1,2,4-triazol-1-ylmethyl)biphenyl, and H_3BTC = 1,3,5-benzenetricarboxylic acid) [12]. The Cu(II) centers are linked to each other by pyrazine ligand into an infinite 1-D chain running along the *a* direction with the intrachain Cu···Cu separation of 6.991 Å (Fig. 2). Moreover, the 1-D chains are linked by intermolecular hydrogen bonds between lattice water moieties, and the oxygen atoms of

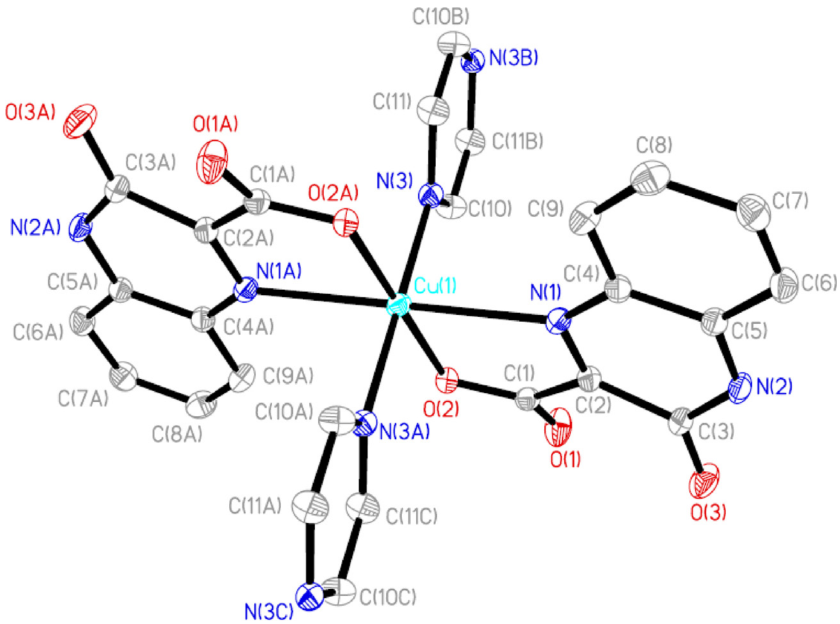

Fig. 1. Coordination environment around the Cu(II) centers in **1**. All H atoms are omitted for clarity.

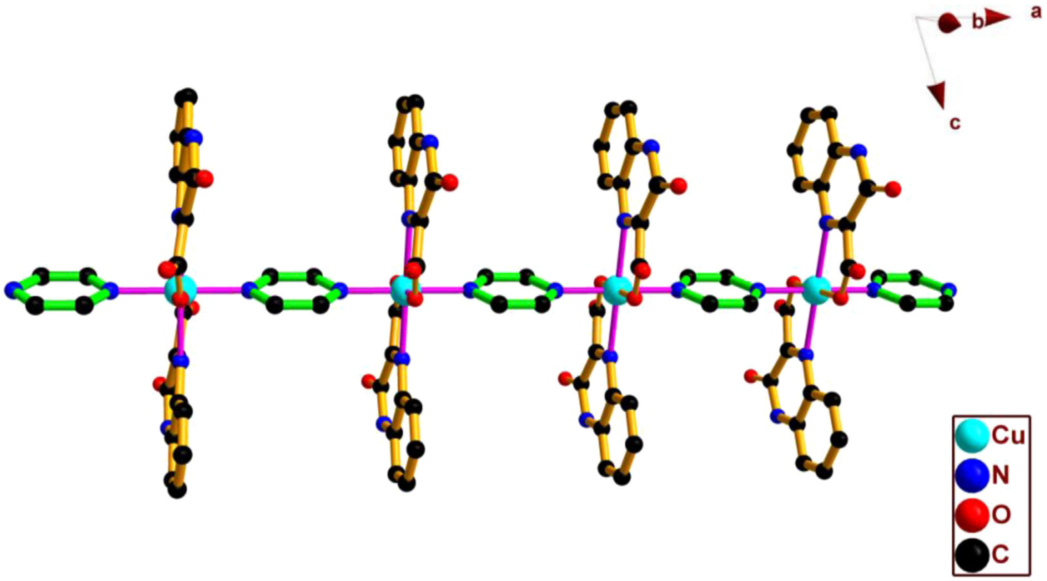

Fig. 2. The 1-D chain structure extending along *a* axis in **1**.

carboxylate and hydroxyl groups from the terminal qc^- ligands to form 2-D ladder chains. These ladder chains are further linked through the interchain hydrogen bonds into a 3-D supramolecular network.

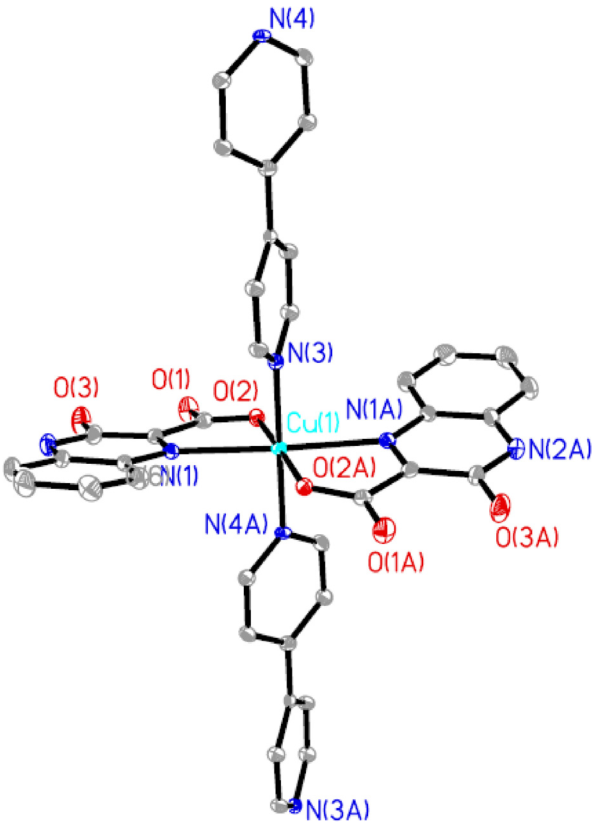

Fig. 3. Coordination environment around the Cu(II) centers in **2**. All H atoms are omitted for clarity.

3.2. Crystal structure of $[Cu(qc)_2(4,4'\text{-bpy})]_\infty$ (2)

Complex **2** crystallizes in the orthorhombic space group Fdd2 with the monomer unit $[Cu(qc)_2(4,4'\text{-bpy})]$. Each Cu(II) atom exhibits a distorted octahedral environment, the equatorial plane of which comprises two carboxylate oxygen atoms and two quinoline nitrogen donors from two distinct qc^- anions and two nitrogen atoms from two 4,4′-bpy ligands occupying the apical site (Fig. 3). The Cu-O/N distances are in the range 1.9901(16)–2.362(2) Å, which are in the normal range of those observed in copper complexes [13]. Each completely deprotonated qc^- ligand serves as a 2-connected node to coordinate with the Cu(II) center. The $[Cu(qc)_2(4,4'\text{-bpy})]$ units are linked into polymeric 1-D chains where 4,4′-bpy connects the adjacent Cu(II) ions of the symmetry related units in an end-to-end bridging mode (Fig. 4). Moreover, the Cu···Cu separation of 11.139 Å within a chain is significantly longer than that of 6.991 Å in **1**. It should be noted that significant aromatic stacking interactions are also observed between the adjacent chain arrays due to the interdigitated disposition. The centroid-to-centroid distance of the alternatively parallel benzene rings in the adjacent chains is 3.289 Å. Two neighboring anti-parallel chains are held together via such weak secondary interactions and C–H···π supramolecular interactions to furnish a 3-D supramolecular framework.

3.3. Crystal structure of $[Cu(pc)(2,2'\text{-bpy})(H_2O)]_2 \cdot H_2O$ (3)

Different from complexes **1** and **2**, in the crystal structure of **3**, the asymmetric unit consists of two Cu^{2+} ions, two 2,2′-bpy ligands, two deprotonated pc^{2-} ions, two coordinated water molecules and one lattice water molecule. Each Cu(II) ion is five-coordinated by two nitrogen atoms of one 2,2′-bpy ligand and three oxygen atoms from two different deprotonated pc^{2-} ligands and

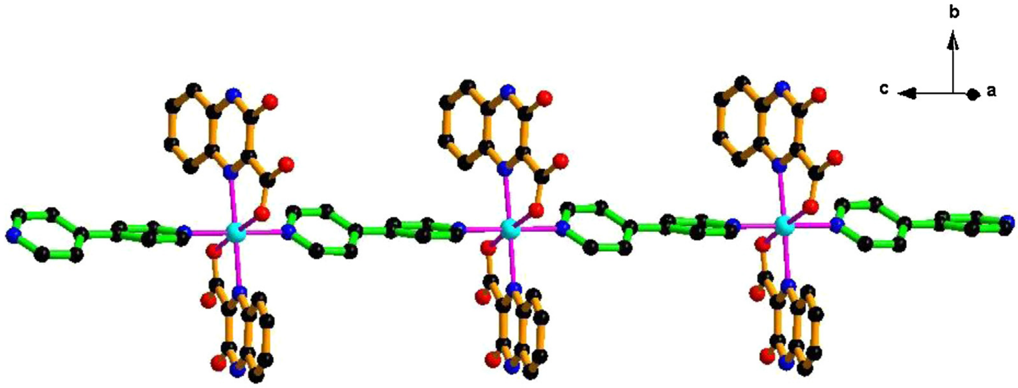

Fig. 4. The 1-D chain structure extending along *c* axis in **2**.

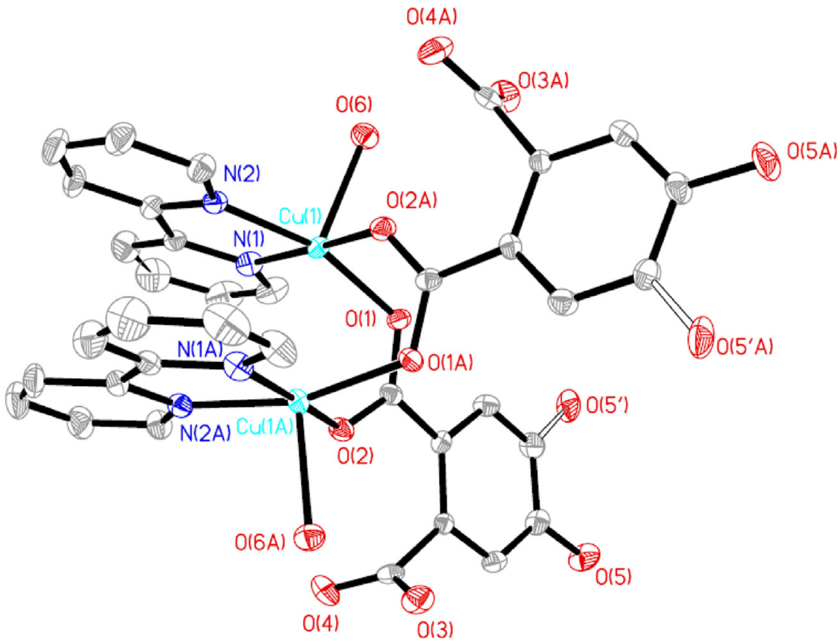

Fig. 5. Molecular structure of **3** with atom labeling of the asymmetric unit. All H atoms are omitted for clarity.

one coordinated water molecule, forming a distorted trigonal bipyramidal geometry, where N1, N2 and O2A locate at the equatorial positions while O6 and O1 occupy the axial positions (Fig. 5). The *d*(Cu–$O_{carboxylate}$) are in the range of 1.952 (2)–1.960 (2) Å, and *d*(Cu–O_{water}) is 2.186 (2) Å, and fall in the range of typical Cu–O (carboxylate and water) distances [14]. The Cu–N bond lengths are 1.992 (3) Å and 1.994 (3) Å. The distorted trigonal bipyramid CuO_3N_2 has the O(N)–Cu–O(N) angles ranging from 81.48 (13)° to 174.41 (12)°, which are within the range expected for such coordination. Each pc^{2-} ligand connects the adjacent Cu(II) centers to form a dimer in a bidentate bridging mode by one of the two carboxylate groups with the Cu···Cu separation of 3.128 Å and another carboxylate group is free of coordination, while the 2,2′-bpy ligand acts as a typical chelating terminally coordinating the Cu(II) center. It is worthwhile to note that hydrogen bonding interactions are usually important in the synthesis of supramolecular architecture. There exist O–H···O hydrogen bonding interactions between lattice water molecules, coordinated water molecule and carboxyl oxygen atoms with the distances in the range of 2.630 (4)–3.40 (2) Å, leading to the formation of a 2-D supramolecular network.

3.4. XRPD results

To confirm whether the crystal structure is truly representative of the bulk materials for related catalytic studies of complexes **1**-**3**, XRPD experiments have been carried out for **1**-**3**. The XRPD experimental and computer-simulated patterns of the corresponding complexes are shown in Fig. 6. Although the experimental patterns have few unindexed diffraction lines and some are slightly broadened in comparison with those simulated from the

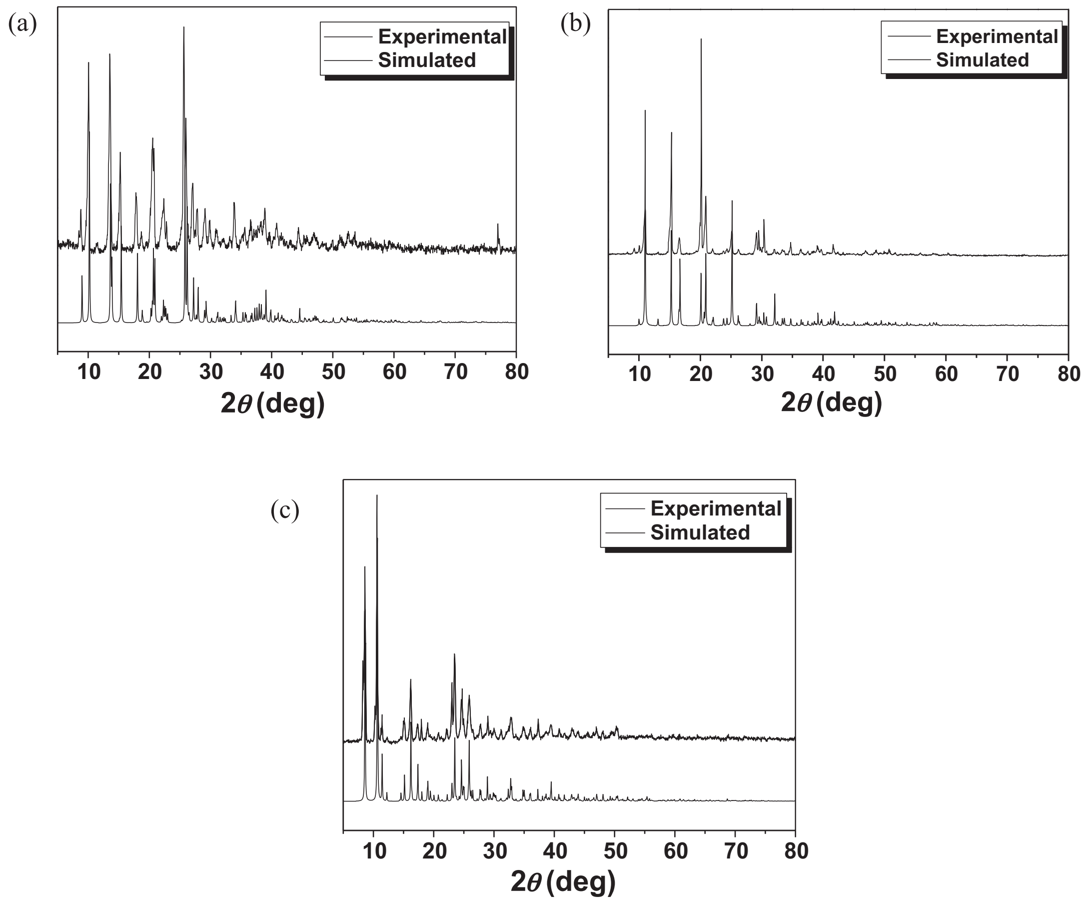

Fig. 6. XRPD patterns of (a) for **1,** (b) for **2** and (c) for **3**.

single-crystal models, it can still be considered that the bulk synthesized materials and the as-grown crystals are homogeneous for **1**-**3**.

3.5. Catalytic oxidative coupling of DMP in water

The overall oxidative coupling process of DMP under green reaction conditions is shown in Scheme 1. Initially, complex **1** was selected as a catalyst model for optimization of the reaction conditions. The influences of various factors such as reaction temperature, reaction time, the amounts of catalyst and oxidant as well as pH of the solution have been investigated in detail.

Previous investigations have indicated that the oxidative coupling of DMP in organic solvents proceeds at room temperature, and higher temperature will result in more by-products DPQ. However, in aqueous media, higher temperature is necessary because the reaction does not proceed at room temperature. Fig. 7 presents the effect of reaction temperatures on the polymerization with **1**, showing a significant temperature effect on the reaction. The DMP conversion increases significantly from 71% to 90% as the temperature increases from 30 to 60 °C, and the best selectivity to PPE of 82.7% is achieved at 45 °C.

In order to study the effect of time on the polymerization, the product analysis was done at regular intervals of

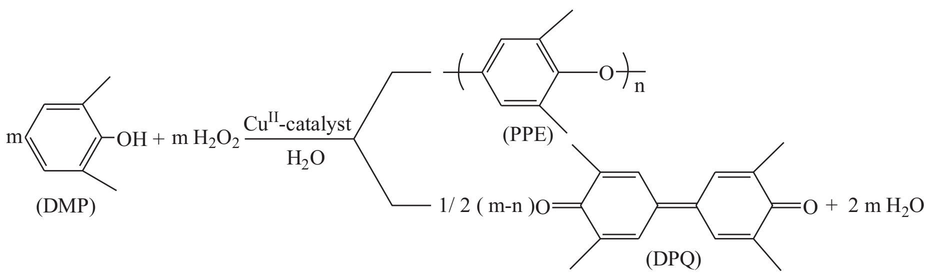

Scheme 1. Oxidative polymerization of 2,6-dimethylphenol (DMP) in water.

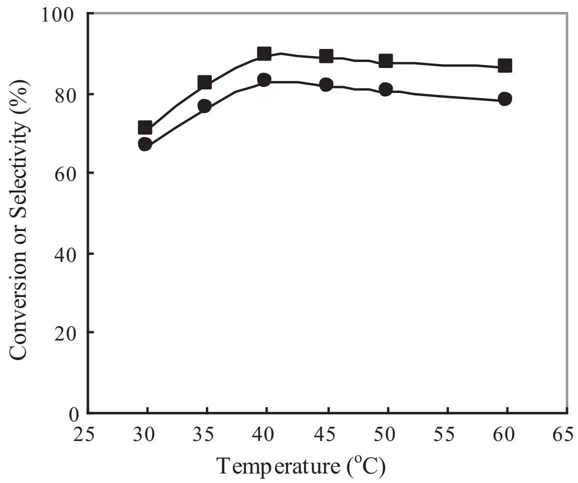

Fig. 7. Effect of reaction temperature on the polymerization with **1**: (■) conversion; (●) selectivity.

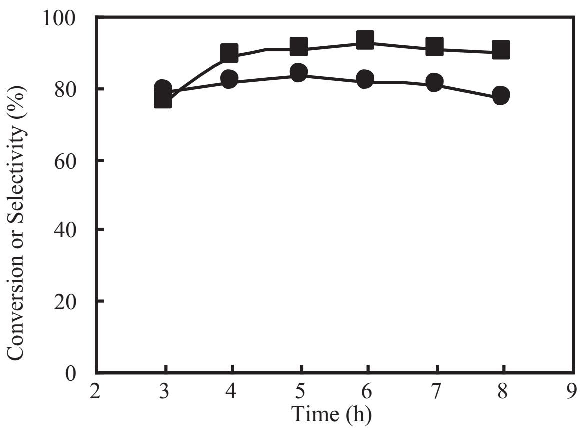

Fig. 8. Effect of reaction time on the polymerization with **1**: (■) conversion; (●) selectivity.

time under similar reaction conditions. DMP conversion increases quickly from about 77% to near 91% as the time changes from 3 h to 8 h, while the selectivity to PPE increases very slowly (Fig. 8). Further prolonging in reaction time does not improve the conversion significantly but decreases the selectivity slightly. The reason for this may be that the by-product DPQ degrades the polymer upon further processing at high temperatures [15]. In addition, we find that the selectivity of PPE is not correlated for the DMP conversion, which is close to an earlier conclusion, since Viersen et al. have shown that most DPQ is formed during the beginning of the reaction [16].

Fig. 9 illustrates the effect of the amount of **1** on the polymerization. The control reaction performed without any catalyst shows that the copper complex is indispensable for the reaction system. The conversion increases with the increased amounts of **1**, but decreases for the larger amounts. The maximum conversion is obtained at a 0.02 mmol amount of **1**. However, the selectivity to PPE keeps stable as the concentration of catalyst increases. The

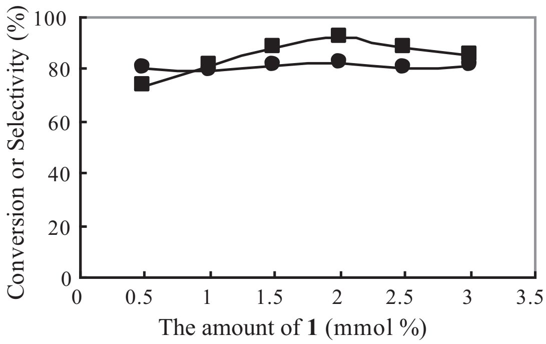

Fig. 9. Effect of the amount of **1** on the polymerization: (■) conversion; (●) selectivity.

decrease in activity at high catalyst concentrations can arise from competitive formation of catalytically inactive copper species. The resultant loss in catalyst concentration will affect the parallel reactions that produce PPE and DPQ equally, and this is consistent with the insensitivity of selectivity to catalyst concentration. The influence of the loading of oxidant is studied by using different volumes of H_2O_2 from 0 to 0.03 mL (30 vol.%). The result indicates that the addition of appropriate amount of H_2O_2 (0.02 mL) is also necessary for obtaining high conversion and selectivity. At higher amounts of H_2O_2, the substrates almost convert completely but the selectivity descends correspondingly, which are similar with the previous results [17].

It has been demonstrated that the pH of solution can affect the yields and the distribution of products [18]. The effect of pH on the DMP polymerization is thus investigated in Tris-HNO_3 buffer solution in the range of pH 6.0–9.0 by maintaining other reaction parameters. As illustrated in Table 3, it can be seen that for the catalytic system with **1**, DMP conversion first increases and then decreases with increasing pH, and the maximum is at pH 7.5. The yield of PPE increases with increasing pH and remains constant above pH 7.5. It is worthy to note that the pH of the solution exhibits great effect on the selectivity of PPE. The selectivity of PPE is less than 82% in a neutral aqueous solution, but about 88% in weakly acidic (pH 6.0) and weakly alkaline (pH 8.5–9.0) solutions. Because of the high conversion of DMP, good yield of PPE and the low loss of H_2O_2 in neutral aqueous solution, optimal pH is around 7.0

Table 3
Effect of pH on the polymerization with **1**[a].

pH	Conversion (%)[b]	PPE (%)[b]	DPQ (%)[b]	Selectivity[c]
6.0	69	62	9	87.8
6.5	78	68	13	84.2
7.0	89	79	18	81.5
7.5	91	82	16	83.5
8.0	88	84	14	85.6
8.5	83	83	12	87.4
9.0	76	83	11	88.1

[a] Standard conditions.
[b] Conversions and isolated yields based on the DMP. All isolated products were identified by ^1H, ^{13}C NMR and IR spectroscopic analyses.
[c] Selectivity = ([PPE] × 100)/([PPE] + [DPQ]).

Table 4
Results of the oxidative coupling of DMP with different catalysts performed under the optimized conditions[a].

Catalysts	Conversion (%)[b]	Yield (%)[b]		Selectivity (%)[c]
		PPE	DPQ	
1	91	75	11	87.2
2	93	82	8	90.9
3	100	94	6	94.4
$Cu(ClO_4)_2$ + Hqc + py	71	26	15	62.7
$Cu(ClO_4)_2$ + Hqc + 4,4′-bpy	68	22	14	61.1
$Cu(ClO_4)_2$ + H_2pc + 2,2′-bpy	69	29	16	64.4
$Cu(ClO_4)_2$	25	9	21	30.0

[a] Optimized conditions: DMP (1 mmol), H_2O_2 (0.02 mL) and catalyst (0.02 mmol) in 5 mL of water for 8 h at 50 °C.
[b] Conversions and isolated yields based on the DMP, average of two runs.
[c] Selectivity = ([PPE] × 100)/([PPE] + [DPQ]).

in practice. The pH effect on product distribution is not entirely clear. It has been reported in the literature that alkaline condition favored the formation of PPE, while acidic solution led to the C–C coupling [19]. However, in this work, both weakly acidic ($pH < 6.5$) and alkaline aqueous solution ($pH > 8$) are suitable to the C–O coupling reaction in our catalytic system. On the basis of the above experimental results and previous literature [20], we think the phenoxy radical associated with metal complex, generated in the reaction process, is the main active species. It is possible that pH of the solution affects the state of metal complex associated with phenoxy radical, consequently influencing the association of the copper complex with phenoxy radical and induction to *p*-C atom.

With the optimized reaction conditions in hand, we then evaluate catalytic efficiencies of the title complexes for comparison. As shown in Table 4, dimer **3** gives relatively high conversion and selectivity of PPE among the three complexes, viz., the conversions and selectivities of 91% and 87.2% for **1,** 93% and 90.9% for **2** as well as 100% and 94.4% for **3**. The dissimilarity is probably attributable to the differences in the coordination environments of the metal Cu(II) centers. In general, a lower coordination number leads to a higher catalytic activity. Also, the coordinated water molecules in the complexes are easy leaving groups and can be readily replaced by the substrate; thus, it is easier for the phenolate anion to enter the metal coordination sphere when metal centers are coordinated by water molecules, further enhancing the catalytic activity. Consistent with our observation, Kol et al. [21] observed that structural effects on reactivity were pronounced in zirconium complexes for lactide polymerization. Comparing with the Cu(II)–poly(N-vinylimidazole), Cu(II)-polyamidoamines complex catalysts giving about 95% PPE yield [22], the best result of the copper-catalyzed synthesis of PPE in aqueous medium so far, complex **3** has an obvious advantage in the oxidative polymerization with the yield of PPE of 94%. However, the contrasting reaction using $Cu(ClO_4)_2$ as catalyst only gives trace amounts of PPE. We also notice that the title complexes have obvious comparative advantage over the $Cu(ClO_4)_2$/Hqc/py, $Cu(ClO_4)_2$/Hqc/4,4′-bpy and $Cu(ClO_4)_2$/H_2pc/2,2′-bpy catalysts under similar reaction conditions. A potential explanation for this may be inferred from the stabilizing effects [17,23] of the organic ligand and the steric influence of the copper center. In **1**-**3**, the bidentate Hqc or H_2pc ligand improves the aqueous stabilities of these complexes and also forms the opening coordination geometry with less steric hindrance around the copper center, which favors the coordination of DMP to Cu(II) to form the proposed active copper species [24] and the subsequent polymerization of DMP. Likewise, Reedijk et al. have also shown that a series of Cu^{II} complexes incorporating structurally related N,O-containing ligands underwent this polymerization more efficiently than copper(II) salts [25].

The potential benefits of the heterogeneous catalyst include facilitation of catalyst separation from reagents and reaction products, and simplification of methods for catalyst recycle [26]. For a truly effective heterogeneous catalyst, therefore, it is critical that recovery can be simple and efficient, and that the recovered catalyst can retain its original reactivity through multiple cycles. As **3** shows higher catalytic activity, we have tested its recovery and reuse. After the reaction was completed, the catalyst was recovered by filtration for consecutive runs. The recovered catalyst was used for a new reaction batch of DMP. Catalyst **3** exhibits excellent reusability for four times without showing any significant deterioration of catalytic activity. Then, we have carried out another control reaction, because in the catalytic process the leached metal species might catalyze efficiently the oxidative coupling reaction instead of the heterogeneous catalysts [27]. To examine this possibility, we filtered catalyst **3** after the oxidative polymerization and allowed the filtered catalyst and the filtrate to react with another aliquot of DMP, respectively, as shown in the previous study [27]. The filtered catalyst was subjected to the second run by charging with new reagents and then the products were again formed with about 85–92% of the original conversion. The filtrate obtained from the first filtration was also used in a new reaction with the addition of substrate. Only 6 to 9% conversion of DMP was observed under similar conditions. This result strongly suggests that the dominant reactive species is the heterogeneous catalyst **3**, not species such as the leached metal. However, about 6–9% conversion by the filtrate indicates that trace amounts of Cu metal ions might be leached during the catalysis. Powder X-ray diffraction (XRD) pattern of the filtered catalyst after the reaction has revealed the same pattern as the original catalyst, suggesting that the original structure of the filtered catalyst has been retained during the reaction. Based on

Table 5
Oxidative coupling of DMP in water[a] or in methanol–toluene mixture[b] catalyzed by complexes **1-3.**

Catalysts	Solvent	Conversion (%)	Selectivity (%)
1	H_2O	91	87.2
	CH_3OH/toluene	68	89.3
2	H_2O	93	90.9
	CH_3OH/toluene	67	91.5
3	H_2O	100	94.4
	CH_3OH/toluene	74	96.3

[a] Heterogeneous optimized conditions: DMP (1 mmol), H_2O_2 (0.02 mL) and catalyst (0.02 mmol) in 5 mL of water for 8 h at 50 °C.
[b] Homogeneous optimized conditions: DMP (1 mmol), NaOMe (0.14 mmol), H_2O_2 (0.05 mL) and catalyst (0.02 mmol) in a 1.5:1 MeOH/toluene mixture for 3 h under the ambient temperature.

these results, we have concluded that the heterogeneous catalyst **3** could be recycled multiple times without a significant loss of activity.

For the purpose of fully understanding the intrinsic advantage of heterogeneous vs. homogeneous catalysts, the oxidation coupling of DMP is conducted in a 1.5:1 (v/v) methanol–toluene mixed solution using complexes **1**-**3** as homogeneous catalysts under the same reaction conditions as the prior study (Table 5) [17a]. To our surprise, the use of the title complexes acting as homogeneous catalysts can effectively suppress diphenoquinone production and improve the selectivity for PPE, while decreasing distinctly the catalytic activities. For example, when utilizing **1** as heterogeneous catalyst, the oxidation coupling of DMP occurs with high 91% conversion and 87.2% selectivity for PPE. Nevertheless, **1** assumes the markedly lower efficiency (68% conversion) for the reaction in methanol–toluene medium, albeit with slightly enhanced selectivity of 89.3%. The superior activities of the complexes in the heterogeneous catalytic system may be attributed to full exposure of metal sites, therefore giving an ultimately high degree of metal-dispersion [28].

On the basis of the above experimental results and previous literature [20,29], a plausible reaction mechanism for the present oxidative coupling reaction was proposed as follows: DMP is dissolved in the basic aqueous phase to form the phenolate anion; these phenoxide anions coordinate to Cu(II) centers, and then an electron transfers from the coordinated phenoxide anions to Cu(II) ions occur, leading to the formation of phenoxyl radicals. The resultant Cu(I) ions were reoxidized to Cu(II) ions by H_2O_2. The C–O coupling of these phenoxyl radicals yields the linear polymer PPE; the C–C coupling of these phenoxyl radicals results in the by-product DPQ.

4. Conclusions

In summary, with the aim of exploiting new and potent catalysts, we have synthesized three mixed-ligand complexes **1**–**3** by the self-assembly of Cu(II) ions with Hqc or H_2pc ligand in the presence of different auxiliary ligands. Using complexes **1**–**3** as catalysts, a green aqueous-medium catalysis process of the oxidative coupling of DMP has been explored with great potential in the aspect of "green chemistry and technology". Recognizing that decreasing the steric hindrance around the copper center should increase the catalytic activity of complex, it can be expected that more studies could improve the catalytic efficiencies via further structural modifications of copper complex for practical application.

Acknowledgments

This work is supported by Scientific Research Foundation for Returned Scholars, Nanjing University of Information Science and Technology (Grant No. S8110247001) and A Project Funded by the Priority Academic Program Development of Jiangsu Higher Education Institutions.

Appendix A. Supplementary material

Supplementary material associated with this article can be found at http://www.sciencedirect.com, at http://dx.doi.org/10.1016/j.crci.2012.11.011.

References

[1] (a) S.S. Han, W.A. Goddard, J. Am. Soc. Chem. 129 (2007) 8422;
(b) T. Kaczorowski, I. Justyniak, T. Lipinska, J. Lipkowski, J. Lewinski, J. Am. Chem. Soc. 131 (2009) 5393;
(c) Y. Yamauchi, M. Yoshizawa, M. Fujita, J. Am. Chem. Soc. 130 (2008) 5832.
[2] (a) J. Xu, Z.R. Pan, T.W. Wang, Y.Z. Li, Z.J. Guo, S.R. Batten, H.G. Zheng, Cryst. Eng. Comm. 12 (2010) 612;
(b) F.W. Zhang, Z.F. Li, T.Z. Ge, H.C. Yao, G. Li, H.J. Lu, Y.Y. Zhu, Inorg. Chem. 49 (2010) 3776.
[3] (a) J.W. Godden, S. Turley, D.C. Teller, E.T. Adman, M.Y. Liu, W.J. Payne, J. LeGall, Science 253 (1991) 438;
(b) N. Kitajima, Adv. Inorg. Chem. 39 (1992) 1;
(c) J.P. Klinman, Chem. Rev. 96 (1996) 2541;
(d) J.L. Pierre, Chem. Soc. Rev. 29 (2000) 251.
[4] A.S. Hay, H.S. Blanchard, G.F. Endres, J.W. Eustance, J. Am. Chem. Soc. 81 (1959) 6335.
[5] K. Saito, T. Masuyama, H. Nishide, Green Chem. 5 (2003) 535.
[6] J.M. DeSimone, Science 297 (2002) 799.
[7] C.J. Li, L. Chen, Chem. Soc. Rev. 35 (2006) 68.
[8] K. Saito, T. Tago, T. Masuyama, H. Nishide, Angew. Chem. Int. Ed. 43 (2004) 730.
[9] A.X.S. Bruker, SAINT Software Reference Manual, Madison, WI, 1998.
[10] G.M. Sheldrick, SADABS, in: Siemens Area Detector Absorption Corrected Software, University of Göttingen, Germany, 1996.
[11] G.M. Sheldrick, SHELXTL NT, in: Version 5. 1; Program for Solution and Refinement of Crystal Structures, University of Göttingen, Germany, 1997.
[12] (a) E.C. Yang, W. Feng, J.Y. Wang, X.J. Zhao, Inorg. Chim. Acta 363 (2010) 308;
(b) Y.J. Mu, J.H. Fu, Y.Y. Song, Z. Li, H.W. Hou, Y.T. Fan, Cryst. Growth Des. 11 (2011) 2183.
[13] (a) E.P. Zhang, H.W. Hou, H.Y. Han, Y.T. Fan, J. Organomet. Chem. 693 (2008) 1927;
(b) M. Du, C.P. Li, X.J. Zhao, Cryst. Growth Des. 6 (2006) 335.
[14] S.S. Sandhu, M.S. Hundal, G. Sood, S.S. Dhillon, J. Chem. Soc. Dalton Trans. (1989) 1341.
[15] P.J. Baesjou, W.L. Driessen, G. Challa, J. Reedijk, J. Mol. Catal. A 110 (1996) 195.
[16] F.J. Viersen, G. Challa, J. Reedijk, Recl. Trav. Chim. Pays-Bas 109 (1990) 97.
[17] (a) B. Xiao, H.W. Hou, Y.T. Fan, J. Organomet. Chem. 692 (2007) 2014;
(b) B. Xiao, H.W. Hou, Y.T. Fan, J. Mol. Catal. A: Chem. 288 (2008) 42;
(c) B. Xiao, L.J. Yang, H.Y. Xiao, S.M. Fang, J. Coord. Chem. 65 (2012) 1398.
[18] Y. Liu, Q.H. Pang, X.G. Meng, F.R. Liu, J.M. Li, J. Du, C.W. Hu, J. Appl. Polym. Sci. 118 (2010) 2043.
[19] H. Higashimura, K. Fujisawa, S. Namekawa, M. Kubota, A. Shiga, Y. Moro-Oka, H. Uyama, S. Kobayashi, J. Polym. Sci. Part A: Polym. Chem. 38 (2000) 4792.
[20] (a) C. Boldron, I.G. Arom, G. Challa, P. Gamez, J. Reedijk, Chem. Commun. (2005) 5808;
(b) J. Gao, J.H. Reibenspies, A.E. Martell, Inorg. Chim. Acta 338 (2002) 157.

[21] S. Gendler, S. Segal, I. Goldberg, Z. Goldschmidt, M. Kol. Inorg. Chem. 45 (2006) 4783.
[22] (a) C. Gu, K. Xiong, B.Q. Shentu, W.L. Zhang, Z.X. Weng, Macromolecules 43 (2010) 1695;
(b) W.L. Zhang, H. Wang, B.Q. Shentu, C. Gu, Z.X. Weng, J. Appl. Polym. Sci. 120 (2011) 109.
[23] H.Y. Han, S.J. Zhang, H.W. Hou, Y.T. Fan, Eur. J. Inorg. Chem. (2006) 1594.
[24] (a) P. Gamez, C. Simons, R. Steensma, W.L. Driessen, G. Challa, J. Reedijk, Eur. Polym. J. 37 (2001) 1293;
(b) S. Tanase, P.M. Gallego, E. Bouwman, G.J. Long, L. Rebbouh, F. Grandjean, R. Gelder, I. Mutikainen, U. Turpeinen, J. Reedijk, Dalton Trans. (2006) 1675.
[25] S.J.A. Guieu, A.M.M. Lanfredi, C. Massera, L.D. Pacho'n, P. Gamez, J. Reedijk, Catal. Today 96 (2004) 259.
[26] Y. Kim, S.K. Choi, S.M. Park, W. Nam, S.J. Kim, Inorg. Chem. Commun. 5 (2002) 612, and references therein.
[27] (a) S.K. Yoo, J.Y. Ryu, J.Y. Lee, C. Kim, S.J. Kim, Y. Kim, Dalton Trans. (2003) 1454;
(b) S.J. Hong, J.Y. Ryu, J.Y. Lee, C. Kim, S.J. Kim, Y. Kim, Dalton Trans. (2004) 2697.
[28] U. Mueller, M. Schubert, F. Teich, H. Puetter, K. Schierle-Arndt, J. Pastre, J. Mater. Chem. 16 (2006) 626.
[29] P.J. Baesjou, W.L. Driessen, G. Challa, J. Reedijk, J. Am. Chem. Soc. 119 (1997) 12590.